

Phonon-assisted tunneling between singlet states in two-electron quantum dot molecules

A. Grodecka,^{1,*} P. Machnikowski,² and J. Förstner¹

¹*Computational Nanophotonics Group, Theoretical Physics,
University Paderborn, 33098 Paderborn, Germany*

²*Institute of Physics, Wrocław University of Technology, 50-370 Wrocław, Poland*

We study phonon-assisted electron tunneling in semiconductor quantum dot molecules. In particular, singlet-singlet relaxation in a two-electron doped structure is considered. The influence of Coulomb interaction is discussed via comparison with a single electron system. We find that the relaxation rate reaches similar values in the two cases but the Coulomb interaction shifts the maximum rates towards larger separations between the dots. The difference in electron-phonon interaction between deformation potential and piezoelectric coupling is investigated. We show that the phonon-induced tunneling between two-electron singlet states is a fast process, taking place on the time scales of the order of a few tens of picoseconds.

I. INTRODUCTION

Coupled quantum dots (QDs), often referred to as quantum dot molecules (QDMs), have recently attracted much attention^{1,2} due to their potential application in various implementations of quantum computation schemes. Specifically, there have been many proposals for employing two-electron spin states in QDMs^{3,4,5}, benefiting from long decoherence times of the spin⁶. For instance, it was suggested to use singlet and triplet states as logical qubit states and to perform quantum computation⁷ and Bell-states measurements⁸. Initialization, control and read-out of the state of two confined electrons in a QDM have already been experimentally demonstrated². Moreover, such structures are proposed for coherent optical manipulation of two-electron states^{9,10}.

Semiconductor QDMs are embedded in a solid state environment, which leads to electron interaction with the phonon reservoir. Combined with the tunneling coupling, which is of vital importance for many proposals of QDM-based quantum computing, this interaction forms a decoherence channel consisting in a transition between the lowest electron states. The presence of this phonon-assisted coupling between the two spatially displaced low-energy states leads to new effects in the physics of QDMs, as compared to individual QDs^{11,12}. Phonon-assisted tunneling has been thoroughly studied in the case of QDMs doped with a single electron^{13,14,15,16}. Also phonon-induced triplet-singlet relaxation (via spin-orbit coupling) has been analyzed¹⁷. However, to our knowledge, spin-conserving relaxation between singlet states of a two-electron system has not been discussed.

In this paper, we analyze phonon-assisted tunneling in a quantum dot molecule consisting of two laterally coupled semiconductor quantum dots. A system doped with two electrons is considered. We study singlet-singlet relaxation, namely the tunneling from a spatially separated state to the state with two electrons in one QD. For a specific GaAs QDM system, phonon-assisted tunneling rates are calculated. We include Coulomb coupling

between electrons and study how it influences the relaxation of electrons in comparison with the case of a QDM doped with a single electron. It is demonstrated that the presence of one electron strongly affects the tunneling of the other. As a result, the rates of the phonon-assisted electron tunneling for the two doping cases (with one or two electrons) differ considerably, which is especially apparent in their dependence on the distance between the constituent QDs. We consider electrons interacting with acoustic phonon modes via deformation potential and piezoelectric couplings and show their distinguished impact on tunneling in QDMs. It is shown that the piezoelectric mechanism resulting from the considerable change of charge distribution is of great importance in the considered system and for some ranges of QDM parameters it is even the dominant contribution to relaxation. We show that the phonon-assisted tunneling is strong in coupled quantum dots and one should be aware of its influence when designing quantum computation schemes in QDMs.

The paper is organized as follows. In Sec. II, we introduce the model describing a quantum dot molecule with the Coulomb interaction and coupling to the phonon environment. Section III contains the results on phonon-assisted tunneling rates for the two systems under consideration. In Sec. IV, we conclude the paper with final remarks. In the Appendix, we summarize the theory of single-electron phonon-assisted tunneling.

II. MODEL

A. Electron states

We consider a quantum dot molecule which consists of two laterally (in x direction) coupled quantum dots [see Fig. 1(a)]. The structure doped with two electrons is studied. The Hamiltonian of the electron subsystem is given by

$$H_e = \frac{\hbar^2}{2m^*} (\nabla_a^2 + \nabla_b^2) + U(\mathbf{r}_a) + U(\mathbf{r}_b) + V(\mathbf{r}_a, \mathbf{r}_b), \quad (1)$$

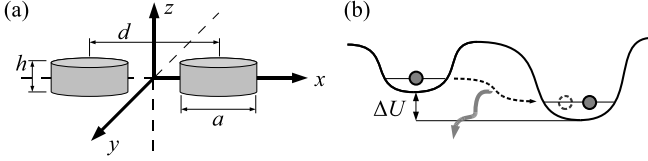


FIG. 1: (a) Schematic plot of a laterally coupled double quantum dot. (b) Scheme of phonon-assisted electron tunneling with confinement potential in x direction.

where $m^* = 0.07m_0$ is the effective mass of an electron in GaAs. $U(\mathbf{r}_{a/b})$ is the confinement potential for two electrons referred to as ‘a’ and ‘b’, respectively, and $V(\mathbf{r}_a, \mathbf{r}_b)$ is the Coulomb interaction between the electrons

$$V(\mathbf{r}_a, \mathbf{r}_b) = \frac{e^2}{4\pi\epsilon_0\epsilon_r} \frac{1}{|\mathbf{r}_a - \mathbf{r}_b|}.$$

Here, e denotes electron charge, ϵ_0 is the vacuum dielectric constant, and ϵ_r is the static relative dielectric constant.

We assume a separable confinement potential

$$\begin{aligned} U(\mathbf{r}) &= U(z) + U(y) + U(x) \\ &= \frac{1}{2}m^*\omega_z^2 z^2 + \frac{1}{2}m^*\omega_y^2 y^2 + U(x), \end{aligned} \quad (2)$$

where $U(z)$ is the potential in the growth direction and $U(y)$ is the lateral confinement potential. The potential describing the double quantum dot structure is $U(x)$ and has two minima, defining the two QDs. We choose it in the form:

$$\begin{aligned} U(x) &= -U_0 \exp \left[-\frac{1}{2} \left(\frac{x - d/2}{a} \right)^2 \right] \\ &\quad - (U_0 + \Delta U) \exp \left[-\frac{1}{2} \left(\frac{x + d/2}{a} \right)^2 \right], \end{aligned} \quad (3)$$

where d is the distance between the dots and a is the width of the quantum dots in the x direction. The confinement depths of the two dots are U_0 and $U_0 + \Delta U$, respectively. The difference between the depths of the two constituent dots ΔU is referred to as the *offset*.

The dynamics in the growth and lateral y directions is restricted to the respective ground states, which are described by Gaussian wave functions

$$\phi(z) = \frac{1}{\sqrt{h\sqrt{\pi}}} \exp \left(-\frac{z^2}{2h^2} \right), \quad (4)$$

$$\varphi(y) = \frac{1}{\sqrt{l\sqrt{\pi}}} \exp \left(-\frac{y^2}{2l^2} \right). \quad (5)$$

Here, h denotes the electron wave function width in growth direction z , while l is the width in lateral direction y . The restriction to the ground states is a reasonable assumption in the considered confinement conditions, since

the energy difference between next eigenstates have typical values larger than 10 meV and do not contribute to the studied dynamics. The complete wave function of a single electron can be written in a product form

$$\Phi_n(\mathbf{r}) = \psi_n(x) \varphi(y) \phi(z), \quad (6)$$

where $\psi_n(x)$ is the n th lowest state of electron in a QDM obtained together with its eigenenergies from the numerical solution of Schrödinger equation. The two lowest single particle eigenstates are described by the wave functions $\Phi_0(\mathbf{r})$ and $\Phi_1(\mathbf{r})$ with the corresponding energies ϵ_0 and ϵ_1 .

In order to analyze the relaxation mechanisms for a system doped with two electrons, we construct two-particle spin-singlet states

$$|\text{RL}\rangle = \frac{1}{\sqrt{2}} \left(a_{0\uparrow}^\dagger a_{1\downarrow}^\dagger + a_{1\uparrow}^\dagger a_{0\downarrow}^\dagger \right) |\text{vac}\rangle, \quad (7)$$

$$|\text{RR}\rangle = a_{0\uparrow}^\dagger a_{0\downarrow}^\dagger |\text{vac}\rangle. \quad (8)$$

Here, $a_{0(1)\uparrow(\downarrow)}^\dagger$ creates an electron in the 0th (1st) lowest single-particle state with spin up (spin down), and $|\text{vac}\rangle$ denotes an empty quantum dot system. The corresponding spatially symmetric wave functions are

$$\Psi_{\text{RL}}(\mathbf{r}_a, \mathbf{r}_b) = \frac{\Phi_0(\mathbf{r}_a)\Phi_1(\mathbf{r}_b) + \Phi_1(\mathbf{r}_a)\Phi_0(\mathbf{r}_b)}{\sqrt{2}}, \quad (9)$$

$$\Psi_{\text{RR}}(\mathbf{r}_a, \mathbf{r}_b) = \Phi_0(\mathbf{r}_a)\Phi_0(\mathbf{r}_b). \quad (10)$$

For the considered two-electron system, we include the Coulomb interaction between electrons, and solve the secular equation in the subspace spanned by the states $|\text{RL}\rangle$ and $|\text{RR}\rangle$, with the projected Hamiltonian

$$\tilde{H} = \begin{pmatrix} \epsilon_0 + \epsilon_1 + v_{00} & v_{01} \\ v_{01} & 2\epsilon_0 + v_{11} \end{pmatrix},$$

where the Coulomb matrix elements are

$$\begin{aligned} v_{00} &= V_0 \int d^3\mathbf{k} \frac{a}{k^2} \{ \text{Re} [\mathcal{F}_{00}^*(\mathbf{k})\mathcal{F}_{11}(\mathbf{k})] + |\mathcal{F}_{01}(\mathbf{k})|^2 \}, \\ v_{01} &= \sqrt{2}V_0 \int d^3\mathbf{k} \frac{a}{k^2} \text{Re} [\mathcal{F}_{00}^*(\mathbf{k})\mathcal{F}_{01}(\mathbf{k})], \end{aligned} \quad (11)$$

$$v_{11} = V_0 \int d^3\mathbf{k} \frac{a}{k^2} |\mathcal{F}_{00}(\mathbf{k})|^2, \quad (12)$$

with

$$V_0 = \frac{e^2}{8\pi^3\epsilon_0\epsilon_r a}.$$

The single-particle form factors are defined as

$$\mathcal{F}_{nm}(\mathbf{k}) = \int d^3\mathbf{r} \Phi_n^*(\mathbf{r}) e^{i\mathbf{k}\cdot\mathbf{r}} \Phi_m(\mathbf{r}) \quad (13)$$

and for our choice of Gaussian wave functions in y and z directions are

$$\begin{aligned} \mathcal{F}_{nm}(\mathbf{k}) &= \exp \left(-\frac{k_z^2 h^2}{4} - \frac{k_y^2 l^2}{4} \right) \\ &\quad \times \int dx \psi_n^*(x) e^{ik_x x} \psi_m(x). \end{aligned} \quad (14)$$

The resulting eigenstates of the interacting system are labeled as $|0\rangle$ and $|1\rangle$ and the corresponding wave functions can be written in the form

$$\begin{aligned}\Psi_0 &= \cos \frac{\alpha}{2} \Psi_{\text{RL}} + \sin \frac{\alpha}{2} \Psi_{\text{RR}}, \\ \Psi_1 &= -\sin \frac{\alpha}{2} \Psi_{\text{RL}} + \cos \frac{\alpha}{2} \Psi_{\text{RR}},\end{aligned}$$

where

$$\alpha = \arctan \left(\frac{v_{01}}{\epsilon_0 - \epsilon_1 + v_{11} - v_{00}} \right),$$

and the energies are E_0 and E_1 , respectively. The splitting between two-electron energies is

$$\Delta E = |E_1 - E_0| = \sqrt{(\epsilon_0 - \epsilon_1 + v_{11} - v_{00})^2 + 4v_{01}^2}.$$

B. Carrier-phonon coupling

In the considered QDM system, carriers not only interact with each other, but are also coupled to phonons.

The free phonon Hamiltonian is

$$H_{\text{ph}} = \sum_{s,\mathbf{k}} \hbar \omega_{s,\mathbf{k}} b_{s,\mathbf{k}}^\dagger b_{s,\mathbf{k}},$$

where $b_{s,\mathbf{k}}^\dagger$ and $b_{s,\mathbf{k}}$ denote phonon creation and annihilation operators, respectively. The corresponding frequencies are $\omega_{s,\mathbf{k}}$, where s labels different phonon branches and \mathbf{k} is the phonon wave vector.

The interaction of the electrons with the phonon reservoir is described by the Hamiltonian

$$H_{\text{int}} = \sum_{nm,\sigma} a_{n,\sigma}^\dagger a_{m,\sigma} \sum_{s,\mathbf{k}} F_{s,nm}(\mathbf{k}) \left(b_{s,\mathbf{k}} + b_{s,-\mathbf{k}}^\dagger \right), \quad (15)$$

where $F_{s,nm'}(\mathbf{k})$ are the single-particle coupling constants [see Eqs. (A.1) and (A.2) in the Appendix], which have the symmetry $F_{s,nm'}(\mathbf{k}) = F_{s,n'n}^*(-\mathbf{k})$, and σ denotes the spin orientation.

We consider the electron tunneling between QDs constituting the QDM, which is a real transition on a picosecond time scale, therefore it can be treated within the Fermi golden rule approach. The coupling between the two considered singlet states in a two-electron configuration, resulting from the carrier-phonon interaction Hamiltonian (15) is

$$H_{\text{int}} = |0\rangle\langle 1| \sum_{s,\mathbf{k}} G_s(\mathbf{k}) \left(b_{s,\mathbf{k}} + b_{s,-\mathbf{k}}^\dagger \right) + \text{h.c.},$$

where $G_s(\mathbf{k})$ are the two-electron coupling constants (given below).

The energy difference between the electron states is considerably smaller than the energy of longitudinal optical phonons (LO), which is 36 meV in GaAs, thus they

will not contribute to the relaxation mechanisms. Therefore, we consider interaction only with the relevant acoustic phonons via the deformation potential and the piezoelectric coupling.

Using the carrier-phonon coupling constant for the deformation potential interaction [Eq. (A.1)], one finds the effective coupling between the two-electron states

$$G_1^{\text{DP}}(\mathbf{k}) = \sqrt{\frac{\hbar k}{2\rho V c_l}} D_e \mathcal{G}(\mathbf{k}),$$

where ρ is the crystal density, V is the normalization volume of the phonon modes, c_l is the longitudinal speed of sound, and D_e is the deformation potential constant for electrons. The geometrical properties of the wave functions are reflected in the form factor $\mathcal{G}(\mathbf{k})$, which has the form

$$\begin{aligned}\mathcal{G}(\mathbf{k}) &= \int d^3\mathbf{r}_a \int d^3\mathbf{r}_b \Psi_0^*(\mathbf{r}_a, \mathbf{r}_b) \\ &\times (e^{i\mathbf{k}\mathbf{r}_a} + e^{i\mathbf{k}\mathbf{r}_b}) \Psi_1(\mathbf{r}_a, \mathbf{r}_b).\end{aligned} \quad (16)$$

It can be written by means of the single-particle form factors defined by Eq. (13) as

$$\begin{aligned}\mathcal{G}(\mathbf{k}) &= \frac{1}{2} \sin \alpha [\mathcal{F}_{00}(\mathbf{k}) - \mathcal{F}_{11}(\mathbf{k})] + \sqrt{2} \cos \alpha \mathcal{F}_{01}(\mathbf{k}) \\ &= \exp \left(-\frac{k_z^2 \hbar^2}{4} - \frac{k_y^2 l^2}{4} \right) \tilde{\mathcal{G}}(k_x).\end{aligned} \quad (17)$$

The two-particle coupling elements for the piezoelectric interaction are

$$G_s^{\text{PE}}(\mathbf{k}) = -i \sqrt{\frac{\hbar}{2\rho V c_s k}} \frac{d_{\text{Pe}}}{\epsilon_0 \epsilon_r} M_s(\hat{\mathbf{k}}) \mathcal{G}(\mathbf{k}), \quad (18)$$

where c_s is the speed of sound (longitudinal c_l or transverse c_t , depending on the phonon branch) and d_{Pe} is the piezoelectric constant. The function $M_s(\hat{\mathbf{k}})$ does not depend on the value of the phonon wave vector, but only on its orientation. For a zinc-blende structure, it reads

$$\begin{aligned}M_s(\hat{\mathbf{k}}) &= \hat{k}_x \left[(\hat{e}_{s,\mathbf{k}})_y \hat{k}_z + (\hat{e}_{s,\mathbf{k}})_z \hat{k}_y \right] \\ &+ \hat{k}_y \left[(\hat{e}_{s,\mathbf{k}})_z \hat{k}_x + (\hat{e}_{s,\mathbf{k}})_x \hat{k}_z \right] \\ &+ \hat{k}_z \left[(\hat{e}_{s,\mathbf{k}})_x \hat{k}_y + (\hat{e}_{s,\mathbf{k}})_y \hat{k}_x \right],\end{aligned} \quad (19)$$

where $\hat{e}_{s,\mathbf{k}}$ is the unit polarization vector for the phonon wave vector \mathbf{k} and polarization s , and $\hat{\mathbf{k}} = \mathbf{k}/k$. We choose the following phonon polarization vectors

$$\begin{aligned}\hat{e}_{l,\mathbf{k}} &\equiv \hat{\mathbf{k}} = (\cos \theta, \sin \theta \cos \varphi, \sin \theta \sin \varphi), \\ \hat{e}_{t1,\mathbf{k}} &= (0, \sin \varphi, -\cos \varphi), \\ \hat{e}_{t2,\mathbf{k}} &= (-\sin \theta, \cos \theta \cos \varphi, \cos \theta \sin \varphi),\end{aligned} \quad (20)$$

for which the functions $M_s(\hat{\mathbf{k}})$ read

$$\begin{aligned} M_1(\hat{\mathbf{k}}) &= \frac{3}{2} \sin \theta \sin(2\theta) \sin(2\varphi), \\ M_{t1}(\hat{\mathbf{k}}) &= -\sin(2\theta) \cos(2\varphi), \\ M_{t2}(\hat{\mathbf{k}}) &= \sin \theta (3 \cos^2 \theta - 1) \sin(2\varphi). \end{aligned} \quad (21)$$

The properties of the phonon environment are represented by phonon spectral density

$$R(\omega) = \frac{1}{\hbar^2} |n(\omega) + 1| \sum_{s, \mathbf{k}} |G_s(\mathbf{k})|^2 \times [\delta(\omega - \omega_{s, \mathbf{k}}) + \delta(\omega + \omega_{s, \mathbf{k}})], \quad (22)$$

where $n(\omega)$ is the Bose distribution function. The deformation potential contribution is

$$\begin{aligned} R^{\text{DP}}(\omega) &= R_0^{\text{DP}} \omega^3 |n(\omega) + 1| \\ &\times \int_0^{2\pi} d\varphi \int_0^\pi \sin \theta d\theta |\tilde{G}(\omega \cos \theta / c_1)|^2 \\ &\times \exp \left[-\frac{\omega^2}{2c_1^2} \sin^2 \theta (l^2 \cos^2 \varphi + h^2 \sin^2 \varphi) \right], \end{aligned} \quad (23)$$

where

$$R_0^{\text{DP}} = \frac{D_e^2}{16\pi^3 \hbar \rho c_1^5}.$$

The piezoelectric term is

$$\begin{aligned} R_s^{\text{PE}}(\omega) &= R_{0,s}^{\text{PE}} \omega |n(\omega) + 1| \int_0^{2\pi} d\varphi \int_0^\pi \sin \theta d\theta \\ &\times |M_s(\hat{\mathbf{k}}(\varphi, \theta))|^2 |\tilde{G}(\omega \cos \theta / c_s)|^2 \\ &\times \exp \left[-\frac{\omega^2}{2c_s^2} \sin^2 \theta (l^2 \cos^2 \varphi + h^2 \sin^2 \varphi) \right], \end{aligned}$$

where

$$R_{0,s}^{\text{PE}} = \frac{d_P^2 e^2}{16\pi^3 \hbar \rho c_s^3 \varepsilon_0^2 \varepsilon_r^2}.$$

Note that the coupling constants for deformation potential and piezoelectric channels have different parity (as functions of \mathbf{k}) so that these two transition channels do not interfere.

In order to study phonon-assisted tunneling, we employ the Fermi golden rule and obtain the tunneling rate

$$w = 2\pi R \left(\frac{\Delta E}{\hbar} \right), \quad (24)$$

which is proportional to the phonon spectral density at the frequency corresponding to the splitting energy ΔE .

The material parameters (corresponding to GaAs quantum dots) and parameters of the QDM system are given in Table I. Moreover, details concerning tunneling processes in a single electron QDM system, which will be used for comparison, are presented in the Appendix.

Deformation potential for electrons	D_e	-8.0 eV
Density	ρ	5360 kg/m ³
Longitudinal sound speed	c_l	5150 m/s
Transverse sound speed	c_t	2800 m/s
Static dielectric constant	ε_r	13.2
Piezoelectric constant	d_P	0.16 C/m ²
Confinement depth	U_0	30 meV
Wave-function width in:		
z-direction	h	4.0 nm
y-direction	l	10.0 nm
x-direction	a	10.0 nm

TABLE I: The GaAs material parameters and QDM system parameters.

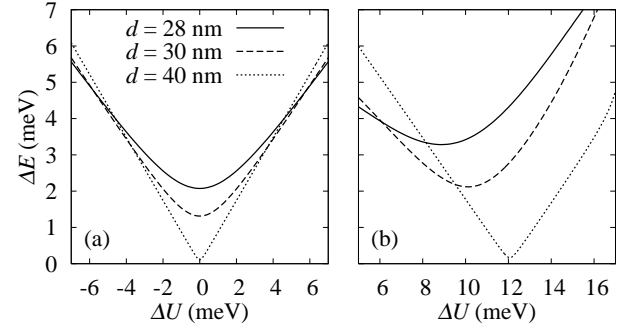


FIG. 2: (a) Splitting energy as a function of the QDs offset for a single electron in a QDM for different distances d between QDs. (b) As in (a) but for two electrons in a QDM.

III. RESULTS: TUNNELING RATES

In this section, the results for phonon-assisted tunneling in a double quantum dot are presented. We consider a QDM doped with two electrons and the singlet-singlet relaxation channel. In order to investigate how the Coulomb interaction influences the tunneling processes, the results are compared with those for a single electron case, calculated in a way similar to Refs. 13,14,15,16 (see Appendix). The quantitative results are obtained at temperature $T = 0$ K for GaAs quantum dots with the sizes $h = 4$ nm and $l = a = 10$ nm in growth and lateral directions, respectively.

The probability of phonon-assisted electron transitions [Eq. (24)] is proportional to the spectral density of the phonon reservoir at the frequency corresponding to the energy splitting ΔE . Therefore, the tunneling rate will be high when this energy lies in the frequency range of maximal values of the phonon spectral density. In order to see which parameter range is favorable for tunneling, we first study the energy splittings and phonon spectral densities for the two considered doping cases.

In Fig. 2(a), we plotted the energy splitting for a single electron in a QDM as a function of the confinement depth offset ΔU for $U_0 = 30$ meV and a few values of the

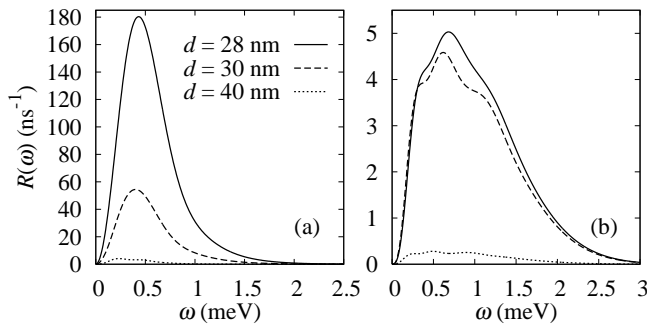


FIG. 3: (a) Total spectral density of the phonon reservoir for one electron in a QDM for $\Delta U = 0$ meV and different distances d between the QDs. (b) As in (a) but for two electrons and $\Delta U = 11$ meV.

distance d between the QDs. The minimum value occurs always when the QDs are the same and in general is smaller for larger distances between dots, where they do not influence each other. In the case of two electrons in a QDM [Fig. 2(b)], the splitting energies have a slightly more complicated behavior. Now, the minimum value is shifted due to interplay between the on-site (single-particle) potential and the Coulomb interaction, which also depends on the distance between QDs. The splitting energies are larger, since they describe two-particle states affected by Coulomb coupling. While for one electron, the energies are symmetric with respect to the offset, in the two-electron case they are not. This will be reflected in the transition rates.

Since the wave functions obviously depend on the confinement offset ΔU , so do the coupling constants and, in consequence, the phonon spectral densities. In order to gain some information on their general shape, we study the spectral densities for the values of the offset which correspond to the minimal values of energy splitting. In Fig. 3(a), the phonon spectral density for a single electron [see Eqs. (A.3) and (A.4) in the Appendix] is plotted for the offset $\Delta U = 0$ meV. In general, the values of phonon spectral densities depend on the overlap between the wave functions and thus are large for small distances d between the QDs. The function has its maximum for $\omega \approx 0.4$ meV and a cut-off at $\omega \approx 2.5$ meV. One can expect high tunneling rates for energy splittings from 0.1 to 1 meV, especially for small distances d . From Fig. 2(a) it is clear that for closely spaced QDs, the energy splitting is larger than 2 meV and lies almost beyond the cut-off of the phonon density, which will result in lower tunneling rates. For larger distances the splitting is smaller, but also the amplitude of the spectral density is smaller. The interplay of phonon density and splitting energies will be reflected in nontrivial dependence of relaxation rates on the distance between the QDs.

For a two-electron QDM, the phonon spectral density has, in general, smaller values [Fig. 3(b)], since the overlap between corresponding two-electron wave functions is smaller. In this case, the cut-off energy ($\omega \approx 3$ meV)

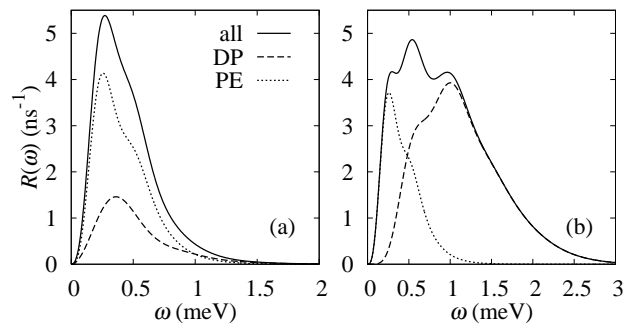


FIG. 4: (a) Total phonon spectral density with the contributions resulting from deformation potential and piezoelectric couplings for one electron in a QDM for $\Delta U = 0$ meV and $d = 38$ nm. (b) As in (a) but for two electrons and $\Delta U = 11$ meV.

as well as the energy splitting is larger. One can see that phonon-assisted tunneling in both systems will be large for energy splittings smaller than 3 meV and will strongly depend on the distance d .

The electron-phonon interaction via both deformation potential as well as piezoelectric coupling is considered next. In order to see which interaction has a stronger influence, in Figs. 4(a) and 4(b) we present the total spectral density of the phonon environment together with the two contributions for a fixed distance $d = 38$ nm. It is clear that piezoelectric coupling in the double quantum dot structures is of great importance in contrast to optical processes in single QD structures, where this interaction can in many cases be neglected^{18,19,20}. This results from the fact that electron tunneling induces a large change of charge distribution. Since in a single electron as well in a two-electron system the two phonon contributions may cover different frequency ranges sectors, they will also play a role in the tunneling rates at distinct parameter areas.

We start the discussion of phonon-assisted tunneling from the deformation potential contribution. For a one-electron QDM [Fig. 5(a)], the rates are symmetric with respect to the offset of the quantum dots ΔU . This results from the symmetric behavior of the splitting energies ΔE . When the QDs are close to each other, $d \lesssim 28$ nm, the tunneling is small, since the energy difference between the two lowest electron states is much larger than the acoustic phonon energies. Thus one-phonon transitions are impossible. For distances d from 28 to 38 nm, the relaxation rate is high. It corresponds to the situation when the energy splittings are comparable to the phonon energies. The transition rate reaches its maximum value of 30 ns^{-1} for $d \approx 32$ nm. Here, the tunneling conditions are most favorable, since the distance between the QDs is large enough for the splitting energy to coincide with the maximum value of the phonon spectral density. For large distances, $d \gtrsim 38$ nm, the tunneling vanishes in spite of small splitting energies, since the overlap between the electron wave functions tends

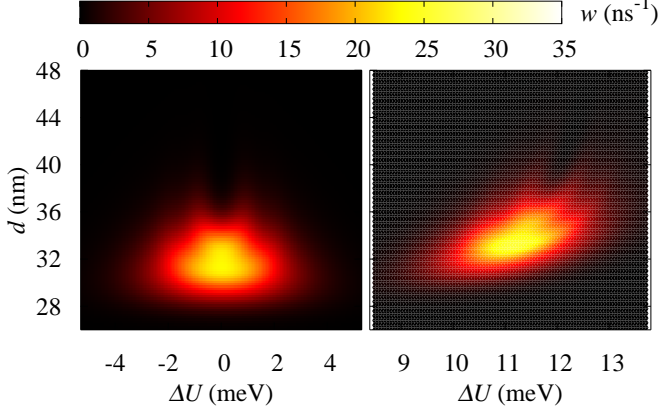


FIG. 5: (a) Electron tunneling rate assisted by phonons via deformation potential coupling for a single electron in a QDM as a function of QDs offset and distance d . (b) As in (a) but for two electrons.

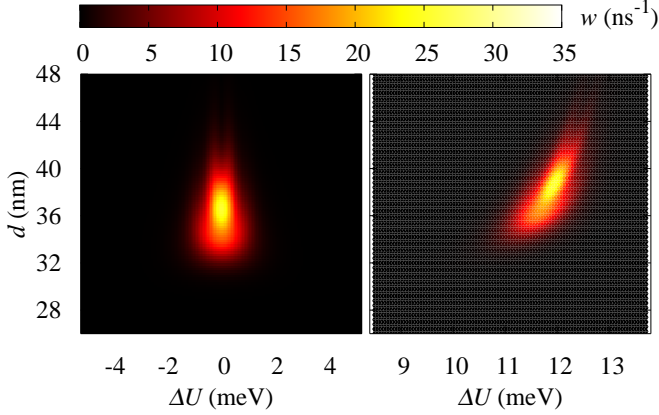


FIG. 6: (a) Electron tunneling rate assisted by phonons via piezoelectric coupling for a single electron in a QDM as a function of QD confinement offset ΔU and distance d . (b) As in (a) but for two electrons.

to zero and, in consequence, the spectral density vanishes. The tunneling rates are also small for large offsets, $|\Delta U| \gtrsim 3$ meV, since it leads to large energy gap between the levels.

For a two-electron QDM [Fig. 5(b)], the maximum of the tunneling rate shifts with growing distance towards larger confinement offsets, which was already visible in the splitting energies. Larger distances d between the QDs are needed for efficient relaxation, which is an evidence of the Coulomb interaction between two electrons, leading to an increase of the splitting energies. In general, the maximum magnitude of the relaxation rates is comparable with that for a single electron but the parameter range in which their values are maximal is shifted due to the electron-electron interaction.

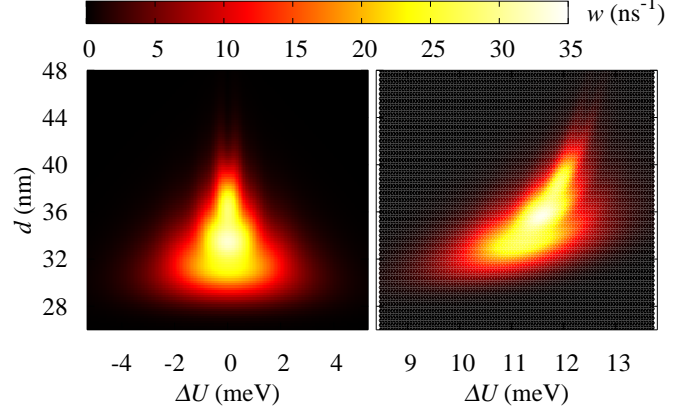


FIG. 7: (a) Relaxation rate for all phonon modes and one electron in a QDM. (b) As in (a) but for two electrons.

In the case of piezoelectric coupling [Figs. 6(a) and 6(b)], the tunneling rate has relatively large values in a smaller range of QD offsets. This is a result of a different form of corresponding spectral density, which, in general, is narrower than for the deformation potential. Therefore, smaller splitting energies are more favorable. For the same reason, it is shifted towards larger distances d . The relaxation rate reaches the values of 30 ns^{-1} , which is as large as that for deformation potential. This maximum appears at the distance $d \approx 36$ nm for a single electron and $d \approx 39$ nm for a double electron QDM.

The total phonon-induced relaxation rate, including both deformation potential as well as piezoelectric contributions, is shown in Figs. 7(a) and 7(b) as a function of QD offset ΔU and separation d . For a single electron system, the tunneling rate is high for offsets between $\Delta U = -3$ and $\Delta U = 3$ meV and for distances from $d = 28$ to $d = 42$ nm, and reaches its maximal value of 35 ns^{-1} for identical QDs separated by the distance of $d \approx 34$ nm. In case of the QDM doped with two electrons, the relaxation mechanism is strong for offsets between $\Delta U \approx 9$ and $\Delta U \approx 13$ meV and distances from $d \approx 30$ to $d \approx 44$ nm. Its maximum value also reaches 35 ns^{-1} for $\Delta U \approx 11.5$ meV and $d \approx 36$ nm.

To have a better insight into particular phonon contributions, in Figs. 8(a) and 8(b) we present the total relaxation rate along with the contributions from both the coupling mechanisms for a two-electron QDM for $d = 35$ nm and $d = 38$ nm, respectively. For relaxation rates of comparable values, the dominant phonon coupling can be different. For instance, for $d = 35$ nm, the deformation potential coupling is crucial and the piezoelectric effect is a few times smaller, while for $d = 38$ nm the situation is reverse.

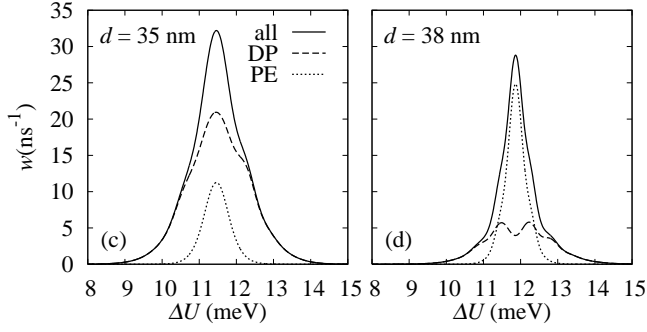


FIG. 8: (a) Total phonon-assisted relaxation rate with two contributions in a two-electron QDM for $d = 35$ nm. (b) As in (a) but for $d = 38$ nm.

IV. CONCLUSION

In the present paper, we have studied phonon-assisted tunneling in a quantum dot molecule. Structures doped with two electrons have been considered and compared with the case of a single electron. By comparison of these two systems, it was shown that the Coulomb interaction influences the tunneling rates and leads to energy renormalization and shift of the range of efficient relaxation. We studied in detail carrier-phonon interactions via both deformation potential and piezoelectric coupling and showed the difference in their behavior and impact on relaxation.

It should be noted that the values of phonon-assisted tunneling rates in a QDM system are comparable with relaxation times in a single QD²¹. Moreover, in comparison with the spin coherence times being up to miliseconds⁶, the phonon-assisted relaxation times are up to several orders of magnitude faster. This shows that while designing the quantum computer implementations on electron states in double quantum dots, one has to take into account the coupling of the carriers to the phonon degrees of freedom. Finally, it should be noted that the calculations were performed for zero temperature, which gives a lower bound for tunneling rates.

Acknowledgments

A. G. and J. F. acknowledge support from the Emmy Noether Program of the Deutsche Forschungsgemeinschaft (Grant No. FO 637/1-1). P. M. acknowledges support from the Polish MNiSW (Grant No. N202 1336 33). P. M. thanks R. Buczko for inspiring discussions.

APPENDIX: SINGLE ELECTRON TUNNELING

In this Appendix, the formalism for the tunneling in a single electron QDM system is presented. In this case,

the electron Hamiltonian [Eq. (1)] is reduced to a simpler form,

$$H_e = \frac{\hbar^2}{2m^*} \nabla^2 + U(\mathbf{r}),$$

and the electrons are described by a single particle wave functions given by Eq. (6). We label the two lowest single electron states as $|\tilde{0}\rangle$ and $|\tilde{1}\rangle$.

The relevant part of the carrier-phonon interaction Hamiltonian describing electron transitions between the constituent QDs is

$$H_{\text{int}} = |\tilde{0}\rangle\langle\tilde{1}| \sum_{s,\mathbf{k}} F_{s,01}(\mathbf{k}) \left(b_{s,\mathbf{k}} + b_{s,-\mathbf{k}}^\dagger \right) + \text{h.c.},$$

where the single-particle coupling constant for the deformation potential is

$$F_{1,01}^{\text{DP}}(\mathbf{k}) = \sqrt{\frac{\hbar k}{2\rho V c_1}} D_e \mathcal{F}_{01}(\mathbf{k}) \quad (\text{A.1})$$

with the form factors given by Eq. (13). The coupling element for piezoelectric interactions reads

$$F_{s,01}^{\text{PE}}(\mathbf{k}) = -i \sqrt{\frac{\hbar}{2\rho V c_s k}} \frac{d_p e}{\varepsilon_0 \varepsilon_r} M_s(\hat{\mathbf{k}}) \mathcal{F}_{01}(\mathbf{k}), \quad (\text{A.2})$$

where the functions $M_s(\hat{\mathbf{k}})$ are given by Eq. (21).

The corresponding phonon spectral densities for a single electron in a QDM are

$$\begin{aligned} R_{1e}^{\text{DP}}(\omega) &= R_0^{\text{DP}} \omega^3 |n(\omega) + 1| \\ &\times \int_0^{2\pi} d\varphi \int_0^\pi \sin\theta d\theta |\tilde{\mathcal{F}}_{01}(\omega \cos\theta/c_1)|^2 \\ &\times \exp \left[-\frac{\omega^2}{2c_1^2} \sin^2\theta (l^2 \cos^2\varphi + h^2 \sin^2\varphi) \right] \end{aligned} \quad (\text{A.3})$$

and

$$\begin{aligned} R_{1e,s}^{\text{PE}}(\omega) &= R_{0,s}^{\text{PE}} \omega |n(\omega) + 1| \int_0^{2\pi} d\varphi \int_0^\pi \sin\theta d\theta \\ &\times |M_s(\hat{\mathbf{k}}(\varphi, \theta))|^2 |\tilde{\mathcal{F}}_{01}(\omega \cos\theta/c_s)|^2 \\ &\times \exp \left[-\frac{\omega^2}{2c_s^2} \sin^2\theta (l^2 \cos^2\varphi + h^2 \sin^2\varphi) \right], \end{aligned} \quad (\text{A.4})$$

where

$$\tilde{\mathcal{F}}_{01}(k_x) = \int dx \psi_0^*(x) e^{ik_x x} \psi_1(x).$$

The Fermi golden rule relaxation rate is then calculated from Eq. (24), using the total spectral density including both relaxation channels.

-
- * Electronic address: anna.grodecka@uni-paderborn.de
- ¹ M. Bayer *et al.*, Science **291**, 451 (2001).
 - ² J. R. Petta *et al.*, Science **309**, 2180 (2005).
 - ³ D. Loss and D. P. DiVincenzo, Phys. Rev. A **57**, 120 (1998).
 - ⁴ S. D. Barrett and T. M. Stace, Phys. Rev. B **73**, 075324 (2006).
 - ⁵ R. Hanson and G. Burkard, Phys. Rev. Lett. **98**, 050502 (2007).
 - ⁶ M. Kroutvar *et al.*, Nature **432**, 81 (2004).
 - ⁷ J. M. Taylor *et al.*, Nature Physics **1**, 177 (2005).
 - ⁸ H. Zhang, G.-P. Guo, T. Tu, and G.-C. Guo, Phys. Rev. A **76**, 012335 (2007).
 - ⁹ C. Emary and L. J. Sham, Phys. Rev. B **75**, 125317 (2007).
 - ¹⁰ H. E. Türeci, J. M. Taylor, and A. Imamoglu, Phys. Rev. B **75**, 235313 (2007).
 - ¹¹ E. A. Muljarov, T. Takagahara, and R. Zimmermann, Phys. Rev. Lett. **95**, 177405 (2005).
 - ¹² E. Rozbicki and P. Machnikowski, Phys. Rev. Lett. **100**, 027401 (2008).
 - ¹³ Z. J. Wu *et al.*, Phys. Rev. B **71**, 205323 (2005).
 - ¹⁴ V. N. Stavrou and X. Hu, Phys. Rev. B **72**, 75362 (2005).
 - ¹⁵ S. Vorojtsov, E. R. Mucciolo, and H. U. Baranger, Phys. Rev. B **71**, 205322 (2005).
 - ¹⁶ V. López-Richard, S. S. Oliveira, and G.-Q. Hai, Phys. Rev. B **71**, 075329 (2005).
 - ¹⁷ J. I. Climente *et al.*, Phys. Rev. B **75**, 081303(R) (2007).
 - ¹⁸ B. Krummheuer, V. M. Axt, and T. Kuhn, Phys. Rev. B **65**, 195313 (2002).
 - ¹⁹ J. Förstner, C. Weber, J. Danckwerts, and A. Knorr, Phys. Rev. Lett. **91**, 127401 (2003).
 - ²⁰ A. Grodecka, C. Weber, P. Machnikowski, and A. Knorr, Phys. Rev. B **76**, 205305 (2007).
 - ²¹ E. A. Zibik *et al.*, Phys. Rev. B **70**, 161305 (2004).